International Journal of Heat and Mass Transfer 52 (2009) 4390–4399

Contents lists available at ScienceDirect

International Journal of Heat and Mass Transfer

journal homepage: www.elsevier.com/locate/ijhmt

Thermomechanical effects on transient temperature in non-conformal contacts experiencing reciprocating sliding motion

Jun Wen, M.M. Khonsari *

Department of Mechanical Engineering, Louisiana State University, 2508 Patrick Taylor Hall, Baton Rouge, LA 70808, USA

ARTICLE INFO

Article history:
Received 4 December 2008
Received in revised form 21 March 2009
Accepted 21 March 2009
Available online 15 May 2009

Keywords:
Thermomechanical effects
Thermomechanical coupling (TMC)
Oscillatory sliding contact

ABSTRACT

A thermomechanical analysis of a semi-infinite elastic solid in contact with a rigid adiabatic sphere subjected to oscillatory sliding motion is conducted to investigate the effects of transient mechanical and thermomechanical loads on the temperature variation in the solid. The interdependent mechanical and thermal analyses are coupled by an iteration scheme using the transfer matrix method combined with the finite element technique. The significance of interaction among heat generation, temperature rise and contact conditions are interpreted in light of numerical results. It is shown that the constraint of the thermal expansion in the indentation direction between the contacting bodies plays a significant role in the increase of contact pressure and heat generation, which in turn affect the temperature rise and thermal expansion.

1. Introduction

Frictional heating and resulting temperature rise at sliding interfaces is of great importance in a wide variety of engineering applications, such as journal bearings, pin joints and automotive brake system. The frictional heat is a function of friction coefficient, sliding velocity and contact pressure. As the frictional heat flows into the contacting bodies, the contact area changes due to thermal expansion, resulting in the change of the contact pressure, which in turn further intensifies the heat generation and temperature. The cycle of frictional heating leading to thermal expansion and higher contact pressures and temperature often becomes unstable and causes component failure. Thermoelastic instability, hot spotting, seizure, cracking and thermal blistering are all in effect a manifestation of unstable thermal runaway brought about as a result of thermomechanical interaction of contacting bodies.

A review of published literature reveals significant advances have been made in the analytical treatment of thermomechanical responses in sliding contact. Pioneering work in this area began by the early contribution of Blok [1] and Jaegar [2] on the treatment of the temperature rise of a semi-infinite body and has continued by many other researchers thereafter. For example, Tian and Kennedy [3], Liu et al. [4] presented the solutions for temperature rise in semi-infinite body with unidirectional sliding motion, and Hirano and Yoshida [5], Wen and Khonsari [6] developed the solutions for the oscillatory sliding case. The thermomechanical analyses of a half space under given heat source with unidirectional sliding motion are presented by Ju and Farris [7], Liu and Wang [8], Martini et al. [9] and Gong and Komvopoulos [10]. In all of these studies, the distributions of the heat sources were decoupled from the mechanical response of the deformed solid. The heat flux was assumed to be unaffected by the mechanical distortion due to the thermal expansion.

To consider the concomitant effects of mechanical and thermal response, Liu and Wang [11,12] developed two- and three-dimensional thermoelastic contact models of two infinitely large surfaces to account for the thermal effects on the mechanical response for steady state heat transfer. They later extended the analysis to a three-dimensional thermomechanical model of nonconforming contact [13]. By performing a fully coupled finite element analysis, Ye and Komvopoulos [14] examined the simultaneous effects of mechanical and thermal surface load on the deformation of elastic–plastic layered media. Gong and Komvopoulos [15] analyzed an elastic–plastic media with patterned surface in contact with a rigid sphere to study the effects of friction coefficient, sphere radius and repetitive sliding on the contact stress and deformation fields.

The great majority of published literature contains very useful information and insight into the temperature and thermomechanical fields in solids due to the unidirectional moving heat sources or sliding rough surfaces. Nevertheless, a comprehensive study of transient temperature variation for an oscillatory sliding contact with the thermomechanical effects is still lacking.

In the current study, a thermomechanical analysis of a semi-infinite elastic solid in contact with a rigid adiabatic sphere subjected to oscillatory sliding motion is conducted to investigate the effects of transient heat transfer and thermomechanical loads

* Corresponding author.
E-mail address: Khonsari@me.lsu.edu (M.M. Khonsari).

0017-9310/$ - see front matter Crown Copyright © 2009 Published by Elsevier Ltd. All rights reserved.
doi:10.1016/j.ijheatmasstransfer.2009.03.047

Nomenclature

A	oscillating amplitude (m)
$\mathbf{A}$	coefficient matrix associated with initial condition
c	specific heat (J/kg K)
$\mathbf{C}$	capacitance matrix
d, d_i	indentation depth and initial indentation depth, respectively (m)
f	oscillating frequency (Hz)
$\mathbf{F}$	heat load vector including heat flux and convection
h	convective heat transfer coefficient (W/m^2 K)
$\mathbf{H}$	exponential matrix
$\mathbf{I}$	identity matrix
k	thermal conductivity (w/m K)
$\mathbf{K}$	conductance matrix
$\mathbf{M}$	coefficient matrix associated with boundary conditions
n	unit normal outward to the boundary Γ
$\mathbf{N}$	vector of shape functions for element
N, N_q, N_h	node number of the model, contact element number, and number of convective surfaces, respectively.
p, p_0	contact pressure and average contact pressure, respectively (N/m^2)
q,$\bar{q}$, q_0	general flux, prescribed boundary condition of heat flux and average flux, respectively, (W/m^2)
Q	total heat generated in the contact interface (W)
t, t_k	time and the time at kth step (s)
T, $\mathbf{T}$, $T^{(0)}$, $\bar{T}$, T_∞	field temperature, vector of field temperature T, initial temperature, prescribed surface temperature, and ambient temperature, respectively (°C)
υ	oscillating velocity (m/s)
$\mathbf{x}$	coordinate vector (x, y, z) (m)
α	thermal expansion (1/K)
κ	thermal diffusivity, $\kappa = k/\rho c$ (m^2/s)
τ	step time (s)
ρ	density (kg/m^3)
δ_{ij}	Kronecker delta
Γ_T, Γ_q, Γ_h	surface Γ with prescribed temperature, heat flux and convection, respectively
μ	friction coefficient
ω	angular frequency (rad/s)
Ω	domain considered

Superscripts

e	element
(k)	iteration number
T	transpose of matrix
-1	inversion of matrix
i	initial value of parameters

on the temperature variation in the solid. The interdependent mechanical and thermal analyses are coupled by an iteration method using the developed transfer matrix method combined with the finite element technique. The analysis provides a practical method for solving problems that involve thermomechanical coupling (TMC) in the oscillatory contact. The significance of interaction among heat generation, temperature rise and contact conditions are interpreted in light of numerical results. Simulation results reveal that the constraint of the thermal expansion in the indentation direction between the contact bodies plays a significant role in the increase of contact pressure and heat generation, which in turn affect temperature rise and thermal expansion.

2. Model development

2.1. Problem definition and finite element model

Consider an elastic semi-infinite solid in contact with an adiabatic rigid sphere shown in Fig. 1. The load W is applied on the sphere. The sphere oscillates back and forth along the x direction on the surface of the half space. Heat is generated in the contact region due to friction. As the frictional heat flows into the semi-infinite solid, the contact area and the distribution of the contact pressure change due to thermal expansion, which in turn influences the heat generation and temperature. Therefore, the semi-infinite solid is subjected to interdependent thermal and mechanical loads along its surface, requiring simultaneous consideration of these elements.

In the present study, the thermal and elastic parts of the contact solution are treated independently and then combined together through a numerical iteration scheme to obtain a thermomechanical solution according to the following procedure:

(i) Thermoelastic analysis is performed to determine the contact pressure and contact area. At the very beginning, the temperature distribution in the solid stays in its initial condition and thus no thermal load is applied.
(ii) Transient heat transfer analysis is conducted by using the contact results from Step i to simulate the temperature distribution in the medium.
(iii) The sphere is moved according to a specified frequency and oscillatory amplitude and Steps i and ii are repeated until either a steady state for temperature is reached or the maximum temperature exceeds 700 °C, indicating the possibility of thermal induced failure by scuffing.

Fig. 2 shows the FEM model for the problem. Due to symmetry, only one half of the sphere and the half space solid are considered. The exactly same mesh is used for both the thermoelastic analysis and the transient heat transfer analysis. The radius of the rigid sphere is 5 mm, and the dimensions of the solid are $11.7 \times 3.15 \times 4$ mm. The model contains 29,176 nodes and 25,895 eight-node hexahedral elements. Very fine mesh is used at the contact surface to catch the high temperature gradient near the heating region and increase the accuracy in the calculation of contact area and contact pressure.

2.2. Nonlinear thermoelastic analysis

The oscillating motion of the sphere is simulated by moving the sphere along the sliding direction in an incremental fashion. At each oscillatory step, a nonlinear thermoelastic analysis for the

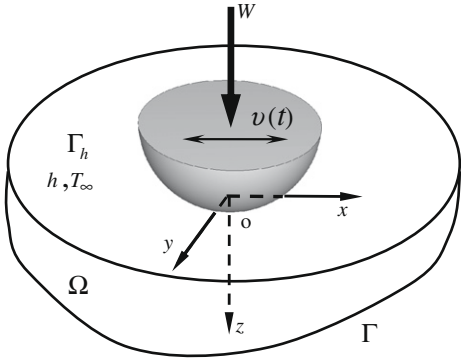

Fig. 1. A semi-infinite body in contact with a rigid ball with oscillatory motion.

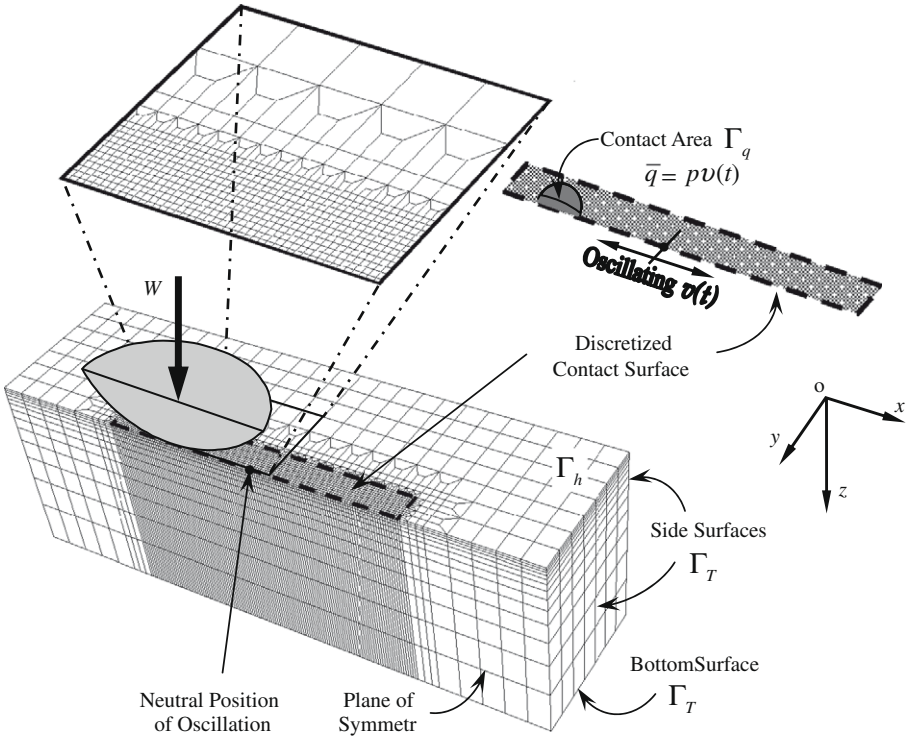

Fig. 2. FEM model of the problem.

contact between the sphere and half space solid is performed by using the finite element method based on the commercial software ABAQUS to determine the contact pressure and the deformation in the solid. The nodes on the bottom surface are fixed against displacement in the x and z directions. The nodes on the symmetric plane are fixed against displacement in the y direction. The sphere is treated as an adiabatic body; therefore, it is only necessary to consider the thermomechanical effects on the semi-infinite solid. Thus, the loads on the contacting bodies include the load on sphere and the thermal load on the semi-infinite body in the form of the nodal temperature obtained by the transient heat transfer analysis. The thermal load results in thermal expansion depending on the material property of the medium. At the first step, there is no temperature variation in the solid and thus no thermal load exists.

In the present study, two types of loads are considered. In the first case, the sphere is oscillating under a constant force W as illustrated in Fig. 1, where the sphere is allowed to move up and down freely depending on the equilibrium between the applied load W and the reaction force in the contact interface, such as in the pin-on-disk device used in a tribometer. In the second case, the sphere is pressed into the semi-infinite solid up to a very small specified depth, d, and oscillates back and forth while keeping the sphere fixed against displacement in the vertical direction. In the contact region, the thermal expansion of the half space along the indentation direction is strictly constrained by the rigid sphere. An example of the second situation is a journal bearing in which the bushing OD is affixed to an external housing. In this case, the thermal expansion of the bushing is constrained by the housing.

2.3. Transient heat transfer by transfer matrix method

The transfer matrix method provides an efficient method to process heat transfer problems in presence of moving heat sources [16]. In this paper, the transient temperature is simulated by the transfer matrix method associated with the finite element method. Since the sphere is treated as an adiabatic body, heat conduction occurs only in the half space solid. In the transient heat transfer analysis, zero temperature is prescribed on the bottom surface and the side surfaces of the solid as shown in Fig. 2. The contact surface is subject to the frictional heating and the rest of the top surface undergoes the convective cooling.

2.3.1. Formulation of the transfer matrix method

The general equation governing a transient temperature field $T(\mathbf{x}, t)$ in a domain Ω with a boundary Γ as illustrated in Fig. 1 or Fig. 2 is:

$$\nabla^2 T(\mathbf{x}, t) = \frac{1}{\kappa}\dot{T}(\mathbf{x}, t), \quad \mathbf{x} \in \Omega, t > 0 \tag{1}$$

with the initial condition

$$T(\mathbf{x}, 0) = T^{(0)}(\mathbf{x}), \quad \mathbf{x} \in \Omega \tag{1a}$$

and the boundary conditions are given by

$$T(\mathbf{x}, t) = \bar{T}(\mathbf{x}, t), \quad \mathbf{x} \in \Gamma_T \tag{1b}$$

$$q(\mathbf{x}, t) = \bar{q}(\mathbf{x}, t), \quad \mathbf{x} \in \Gamma_q \tag{1c}$$

$$q(\mathbf{x}, t) = h(T_\infty - T), \quad \mathbf{x} \in \Gamma_h \tag{1d}$$

where $\mathbf{x}$ is coordinate vector (x, y, z). The parameter t denotes the time, and the super-dot stands for the derivative with respect to time. Parameters κ and k are the thermal diffusivity and the thermal conductivity of the material, respectively. The heat flux $q(\mathbf{x}, t)$ is defined as $q(\mathbf{x}, t) = k\frac{\partial T}{\partial n}$, where n is the unit normal outward to the boundary Γ. The parameter $T^{(0)}(\mathbf{x})$ represents the initial temperature distribution. $\bar{T}(\mathbf{x}, t)$ and $\bar{q}(\mathbf{x}, t)$ are the prescribed boundary temperature on surface Γ_T and heat flux on surface Γ_q, respectively. The boundary surface Γ_h is subjected to convective cooling with the heat transfer coefficient h, and the ambient temperature T_∞.

Using the standard finite element discretization procedure [17,18], Eq. (1) yields the following system of equations in the matrix form as

$$\mathbf{C}\dot{\mathbf{T}}(t) + \mathbf{K}\mathbf{T}(t) = \mathbf{F}(t) \tag{2}$$

where

$$\mathbf{C}=\sum_e \int_{\Omega^e} \mathbf{N}^T \rho c \mathbf{N} d\Omega \tag{2a}$$

$$\mathbf{K}=\sum_e \int_{\Omega^e} \left(\frac{\partial \mathbf{N}^T}{\partial x}k\frac{\partial \mathbf{N}}{\partial x}+\frac{\partial \mathbf{N}^T}{\partial y}k\frac{\partial \mathbf{N}}{\partial y}+\frac{\partial \mathbf{N}^T}{\partial z}k\frac{\partial \mathbf{N}}{\partial z}\right)d\Omega+\sum_e \int_{\Gamma_h^e} h\mathbf{N}^T\mathbf{N}d\Gamma \tag{2b}$$

$$\mathbf{F}=\sum_e \int_{\Gamma_q^e} \bar{q}\mathbf{N}^T d\Gamma+\sum_e \int_{\Gamma_h}^e hT_\infty \mathbf{N}^T d\Gamma \tag{2c}$$

where $\mathbf{N}$ is the shape function in the element of e. Ω^e and Γ^e denote the element domain and the element surface if it is on the boundary, respectively. Parameters ρ and c represent the density and specific heat of the material, respectively. The superscript T denotes the matrix transpose.

Solving Eq. (2) yields the following iteration equation for the heat transfer analysis as

$$\mathbf{T}^{(k+1)}=\mathbf{A}\mathbf{T}^{(k)}+\mathbf{M}\mathbf{F}^{(k)} \tag{3}$$

with

$$\mathbf{A}=e^{\mathbf{H}\tau} \tag{3a}$$

$$\mathbf{M}=(\mathbf{I}-\mathbf{A})\mathbf{K}^{-1} \tag{3b}$$

and

$$\mathbf{H}=-\mathbf{C}^{-1}\mathbf{K} \tag{3c}$$

where the superscript k represents the time step and τ is the time period from time t_k to t_{k+1}. $\mathbf{A}$ and $\mathbf{M}$ are the coefficient matrices and $\mathbf{I}$ is the identity matrix. The superscript -1 denotes the matrix inversion. $\mathbf{F}$ is the vector of the discretized heat load. For a model having N nodes, N_h convective surfaces, and with the contact surface divided into N_q small segmented elements, the dimension of vector $\mathbf{T}$ is N, the dimension of vector $\mathbf{F}$ is $N_h + N_q$, and the dimensions of matrices $\mathbf{A}$ and $\mathbf{M}$ are $N \times N$ and $N \times (N_h + N_q)$, respectively.

Physically, the coefficient matrix $\mathbf{A}$ demonstrates how heat conducts inside the solid, and the coefficient matrix $\mathbf{M}$ shows how the surface heat input contributes to the field temperature rise in the solid. The load vector $\mathbf{F}$ includes two parts. One of them contains the terms involved with the heat flux on the contact surface due to the frictional heating and convective cooling. The other part consists of the terms of the ambient temperature on the convective boundary surfaces. In the present method, except $\bar{q}$ and T_∞, the other terms in Eq. (2c) are multiplied into the corresponding columns of matrix $\mathbf{M}$ in Eq. (3). Therefore, vector $\mathbf{F}$ in Eq. (3) only contains the values of the heat fluxes, corresponding to each small surface element on the discretized contact surface, and the ambient temperatures corresponding to the boundary surfaces subjected to convective cooling. The heat flux on each small surface element is evaluated by the following Eq. (4).

$$q=\begin{cases}\bar{q} & \text{Elements} \in \text{Contact region}\\ h(T_\infty - T) & \text{Elements} \notin \text{Contact region}\end{cases} \tag{4}$$

where the parameter T represents the average temperatures of small segmented elements on the contact surface. Whether a surface element lies inside the contact region or not is determined by the contact pressure obtained in the thermoelastic analysis. If the contact pressure is not equal to zero, the corresponding surface element is in contact with the sphere and the frictional heat $\bar{q}$ is applied on it, otherwise, the surface is not in contact with the sphere and undergoes the convective cooling.

For a sinusoidal oscillation of the heat source in the form of

$$v(t)=A\omega\sin(\omega t) \tag{5}$$

with

$$\omega=2\pi f \tag{5a}$$

where f is the oscillating frequency and A is the oscillating amplitude.

If all the heat dissipated in the frictional contact is converted into heat, the frictional heat flux and the total heat generated in the contact interface can be given as Eqs. (6a) and (6b), respectively.

$$\bar{q}=\mu p A\omega|\sin(\omega t)| \tag{6a}$$

$$Q=\mu W_c A\omega|\sin(\omega t)| \tag{6b}$$

where μ denotes the friction coefficient. p is the contact pressure and W_c represents the contact force.

2.3.2. Calculation of the coefficient matrices

The calculation of the coefficient matrices $\mathbf{A}$ and $\mathbf{M}$ is based on using the commercial software ABAQUS. Examination of Eq. (3) reveals that matrices $\mathbf{A}$ and $\mathbf{M}$ can be treated as *influence matrices*. Each of the column vectors of matrix $\mathbf{A}$ reflects how a unit nodal temperature affects the field temperature inside the solid, and each of the column vectors of matrix $\mathbf{M}$ reflects how a unit discretized boundary flux or unit ambient temperature contributes to the field temperature rise. Thus, in this paper, matrices $\mathbf{A}$ and $\mathbf{M}$ are indirectly calculated by using Eq. (3). The method is described as follows.

The matrix $\mathbf{A}$ can be obtained by N cycles of simulations with the same time period τ. For the ith ($i = 1, 2, \ldots, N$) simulations, the initial condition and boundary load are set to

$$(\mathbf{T}^{(0)})_i=\{\delta_{ij}\} \quad \text{and} \quad \mathbf{F}=\{0\} \tag{7}$$

where δ_{ij} is the Kronecker delta, and $j = 1, 2, \ldots, N$, are the index to the entries of the vector $\mathbf{T}^{(0)}$. The result $\mathbf{T}^{(1)}$ is the ith column of matrix $\mathbf{A}$.

Similarly, the matrix $\mathbf{M}$ can be evaluated by performing $N_h + N_q$ cycles of simulations with the same time period τ as that used in calculation of matrix $\mathbf{A}$. For the ith ($i = 1, 2, \ldots, N_h + N_q$) simulations, the following initial condition and boundary load are applied

$$\mathbf{T}^{(0)}=\{0\} \quad \text{and} \quad (\mathbf{F})_i=\{\delta_{ij}\} \tag{8}$$

where $j = 1, 2, \ldots, N_h + N_q$ are the index to the entries of the vector $\mathbf{F}$. The result $\mathbf{T}^{(1)}$ is the ith column of matrix $\mathbf{M}$.

After $N + N_h + N_q$ cycles of simulations, the coefficient matrices $\mathbf{A}$ and $\mathbf{M}$ are obtained. It is noted that $\mathbf{A}$ and $\mathbf{M}$ keep constant for different heat sources and need to be calculated only once. Once they are determined, the transient temperature distribution in the half space at each time step t_k is easily calculated from Eq. (3). The procedure is to start from the initial condition $\mathbf{T}^{(0)}$ and to assign different values of heat fluxes to the components of vector $\mathbf{F}^{(k)}$ at each time step t_k. This can be evaluated by Eq. (4), according to the oscillatory motion of the sphere, which have been evaluated in the thermoelastic analysis. The final temperature is normalized using the following relationship.

$$\hat{T}=\frac{Tk}{2Rq_0} \tag{9}$$

where R is the contact radius. $q_0 = \mu p_0 A\omega$. The parameter p_0 is the average contact pressure. For thermoelastic analysis, p_0 and R will be the initial contact pressure and corresponding contact radius due to the indentation, respectively.

3. Solution algorithm

A computer program is developed using the procedure described in Sections 2.1–2.3. Fig. 3 presents the flow chart of the basic steps of the simulation algorithm. First, the coefficient matrices $\mathbf{A}$ and $\mathbf{M}$ are evaluated. Then, beginning with a static thermoelastic analysis with consideration of thermal expansion (except in the

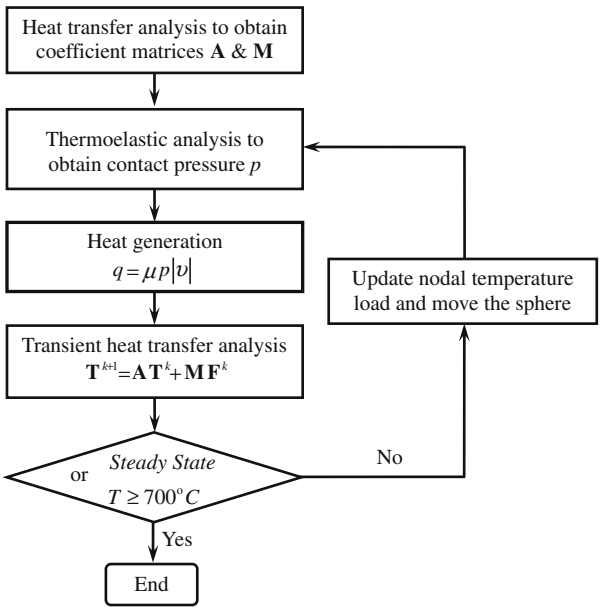

Fig. 3. Flow chart of the basic steps of the simulation algorithm.

first iteration, where is no temperature change and thus no thermal expansion), the results of contact pressure are used to calculate the heat flux by Eq. (6a), which is assigned to the corresponding components of the load vector **F** according to Eq. (4). At the same time, using the temperature result at the previous step as the pseudo-initial temperature or using the initial condition for the first step, the transient temperature after one cycle with the time period τ is obtained by solving Eq. (3). The thermomechanical response in the semi-infinite solid is simulated by moving the sphere according to the specified oscillating motion, updating the nodal temperature load in the semi-infinite solid, and repeating the thermoelastic analysis followed by a thermal analysis, until either a steady state for temperature is reached or the maximum temperature exceeds 700 °C, indicating scuffing failure.

4. Model validation

To evaluate the accuracy of the present model, a normal contact and an oscillatory sliding heat source are simulated. Table 1 lists the parameters used in the simulations. Fig. 4(a) shows the comparison between the finite element results and Hertz analytical solution [19] for an elastic half space indented by a rigid sphere under different loads. The contact pressure is normalized by the maximum Hertz contact pressure $(P_m)_{Hertz}$ and the coordinate by Hertz contact radius R_{Hertz}. Both results are in good agreement.

If the sphere oscillates back and forth along the surface of the half space according to Eq. (5), the contact pressure shown in Fig. 4(a) yields a parabolic heat source described by the following expression.

$$q(r,t) = \frac{3}{2} q_0 (1 - r^2/R^2)^{1/2} |\sin(\omega t)| \tag{10}$$

where R is the contact radius. q_0 is the average heat flux as

$$q_0 = \frac{\mu W A \omega}{\pi R^2} \tag{10a}$$

Without thermomechanical consideration, and with the origin of the coordinate system set at the neural position of the oscillatory motion, the transient temperature at a point (x, y, z) for a parabolic heat source, Eq. (10), oscillating along the x direction according to Eq. (5) on the surface of a half spaces is given in [6] as:

$$T(x,y,z,t) = \frac{3q_0}{8\rho c(\pi\alpha)^{3/2}} \int_{\tau=0}^{t} \frac{|\sin(\omega(t-\tau))| d\tau}{\tau^{3/2}} \int_{\theta=0}^{2\pi} \int_{r=0}^{R} (1-(r/R)^2)^{1/2} \exp \times \left(-\frac{[x - A\cos(\omega(t-\tau)) - r\cos(\theta)]^2 + (y - r\sin(\theta))^2 + z^2}{4\alpha\tau} \right) r dr d\theta \tag{11}$$

The temperature distribution of a half space under a oscillating parabolic heat source in Eq. (10) is simulated using the present transfer matrix method. The result is compared with the analytical solution by Eq. (11) from Ref. [6]. Fig. 4(b) presents the comparison of the surface temperature distributions along the oscillating direction as obtained by the present method and those by Eq. (11) when the temperature at the oscillatory center reaches its maximum value. In this figure, as well as in the subsequent figures, the temperature is normalized by $2Rq_0/k$, and the coordinate is normalized by the contact radius R. It can be seen from Fig. 4(b) that both results are in good agreement.

Favorable comparisons of the results shown in Fig 4 with the analytical solutions indicate the suitability of the finite element model and appropriateness of the presented method for the thermomechanical analysis of the problem proposed in Section 2.

Table 1
Parameters used in the analysis.

Density, ρ (kg/m^3)	7865
Specific heat, c (J/kg K)	460
Thermal conductivity, k (W/m K)	58
Elastic modulus, E (GPa)	200
Poisson ratio, v	0.3
Thermal expansion, a (1/K)	1.15×10^{-5}
Heat transfer coefficient, h (W/m^2 K)	40
Oscillating frequency, f (Hz)	10
Oscillating amplitude, A (mm)	2.0
Friction coefficient, μ	0.2

5. Results and discussion

In this section, the thermomechanical response of the semi-infinite solid in contact with a sphere oscillating back and forth is studied. Two types of loads on the sphere are considered: constant applied force, W = 1000 N, and fixed the displacement of the sphere in the vertical direction after pressing it into the semi-infinite solid up to a very small specified depth. Both loads on the sphere yield the same contact condition at the initial time; that is, the same distribution of contact pressure in the same contact area. During the oscillation, the sphere in the first case is allowed to move freely in the vertical direction depending on the equilibrium between the applied force and the resulted contact force. But in the second case, the sphere is fixed against displacement in the vertical direction. An example of first case is commonly met in a typical pin-on-disk device used in the tribology research laboratory. There are also many applications that experience conditions that can be modeled as the second case such as a journal bearing with its bushing fixed inside an external housing in the manner that its thermal expansion is constrained.

The results for the heat transfer analysis without the thermomechanical interaction are presented to establish a reference for comparison with the results of the thermomechanical analysis. The semi-infinite solid in the heat transfer analysis without the thermomechanical interaction is subjected to the same oscillatory heat source on its top surface as the initial frictional heat flux in the thermoelastic cases. Both cases are simulated until the steady state temperature is reached. The steady state temperature results correspond to the maximum temperature rise in the solid. In the

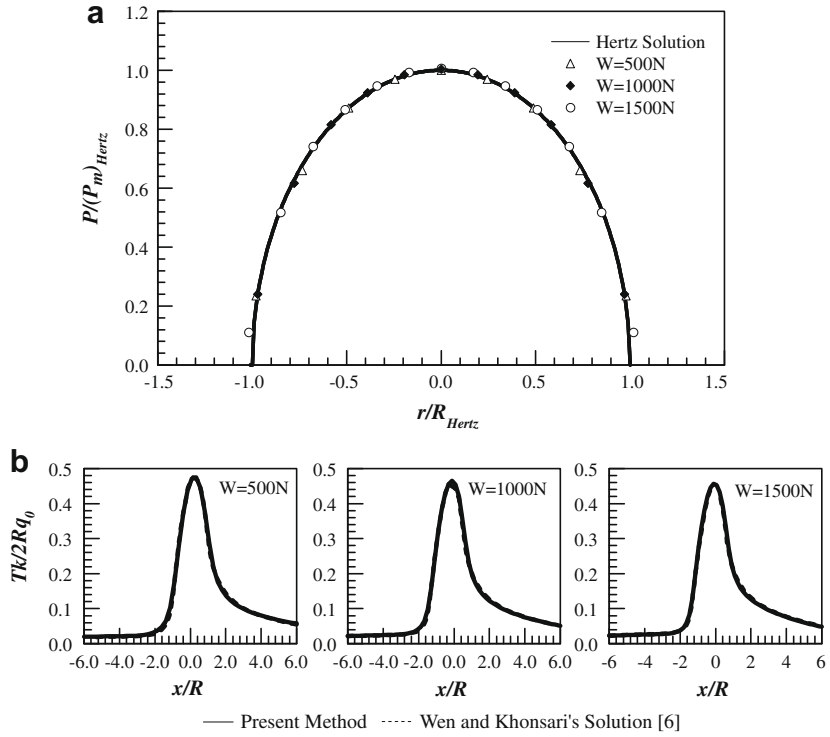

Fig. 4. (a) Comparison of normalized contact pressure for different loads between finite element and Hertz solutions. (b) Comparison of temperature distribution along x direction through the center of the heat source by the present transfer matrix method and the analytical solution. R is the contact radius. q_0 is the average heat flux.

presented study, a steady state condition is assumed once the change in the maximum temperature, computed between consecutive cycles, is less than 10^{-4}. For the periodic oscillatory contact, the temperature result when the sphere or the frictional heat source oscillates from the extreme left to the extreme right is symmetric with corresponding result when the sphere oscillates from the extreme right to the extreme left along the axis through the oscillatory center and perpendicular to the sliding direction. Therefore, only the results corresponding to sphere oscillating from the left to the right are presented in the following Case I and II. The same parameters listed in Table 1 are used.

5.1. Case 1. Oscillatory contact under constant load

In this case, the sphere oscillates along the x direction in contact with a semi-infinite solid under the constant load $W = 1000$ N as illustrated in Fig. 2. The sphere can move freely in the vertical direction depending on the contact force. The results are compared with those for the heat transfer without the thermomechanical consideration.

Fig. 5(a) shows the dimensionless temperature contour for the heat transfer without thermomechanical interaction. Fig. 5(b) includes thermomechanical coupling. Fig. 5 illustrates that the contact temperature is slight higher when the thermomechanical interaction is taken into account. The same characteristic is illustrated in Fig. 6. Fig. 6(a) presents the comparison of the surface temperature distributions along the sliding direction with and without TMC when the sphere oscillates to the five different locations, $x_R = -A$, $-0.5A$, 0, $0.5A$, A, from the left to the right. Fig. 6(b) shows more clearly the distribution of the contact temperature when the sphere is at the oscillatory center. It can be seen from Figs. 5 and 6 that the thermal expansion in Case I only has a little effect on the temperature rise in the contact region, a slight rise and small shift of the maximum contact temperature to the left as shown in Fig. 6(b). The slight increase of the maximum contact temperature due to the thermal expansion becomes negligible when the sphere oscillates to the locations at or near both oscillatory ends as shown in Fig. 6(a).

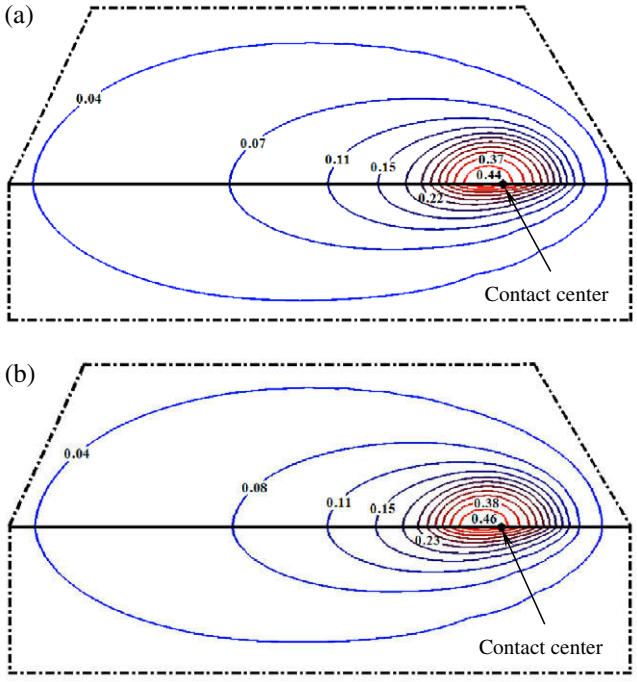

Fig. 5. Dimensionless temperature contours when the heat source/sphere oscillates to the oscillatory center from the left to the right at steady state. (a) Oscillatory contact without TMC. (b) Oscillatory contact under constant applied force with TMC. The temperature is normalized by $2Rq_0/k$. R and q_0 are the initial contact radius and the initial average heat flux, respectively.

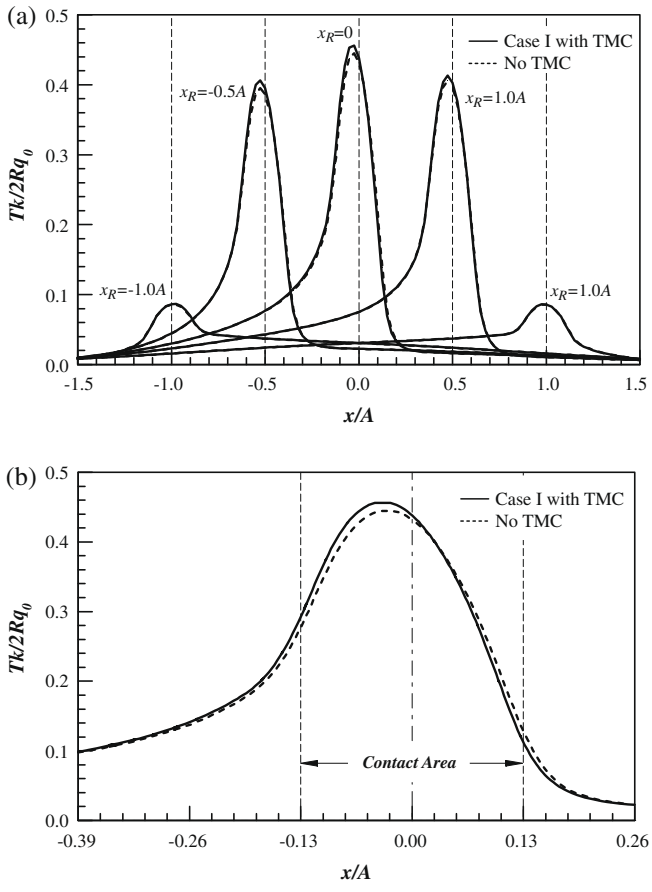

Fig. 6. Comparison of the surface temperature distributions of Case I along with the heat transfer results without TMC along the sliding direction. (a) When the sphere/heat source is at the different locations. (b) When the sphere/heat source is at the oscillatory center. The origin is located at the neutral position of the oscillatory motion. q_0 is the initial average heat flux. A is the oscillatory amplitude.

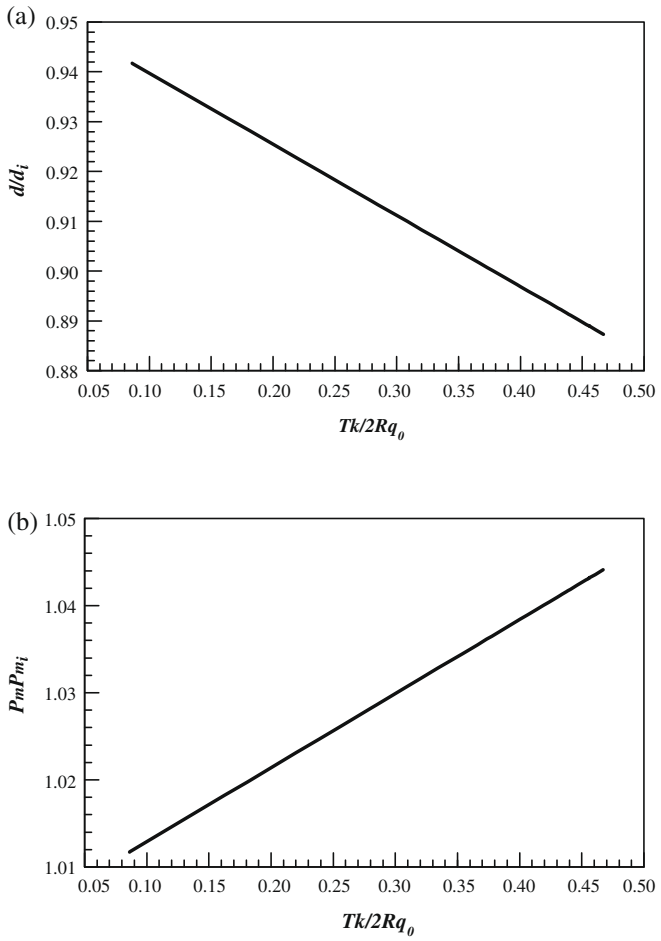

Fig. 7. Variation of (a) indentation depth and (b) maximum contact pressure with the dimensionless maximum contact temperature for the oscillatory contact under constant applied force in Case I. p_{mi} and d_i is the initial maximum contact pressure the initial indentation depth, respectively. R and q_0 are the initial contact radius and the initial average heat flux, respectively.

Fig. 7 shows that the variation of the indentation depth or the downward displacement of the sphere and the maximum contact pressure with the dimensionless maximum contact temperature, respectively. The initial indentation depth d_i and the initial maximum contact pressure p_{mi} are used to normalize the indentation depth and the pressure, respectively. Fig. 7(a) reveals a linear decrease in the indentation depth with the maximum contact temperature to values less than its initial value. Fig. 7(b) demonstrates a linear increase in the peak contact pressure with the maximum contact temperature to values greater than its initial value.

In the case of the oscillatory contact under the constant load W, the thermal expansion due to the temperature rise in the half space results in an outward expansion of the contact surface. This outward expansion of the contact surface "lifts" the sphere up, reduces the indentation depth as shown in Fig. 7(a) and leads to a slight decrease of the contact area. The simulation results reveal that the thermal expansion of the half space results in a decrease of the contact area by 3.8%, except at the locations close to both oscillatory ends where the contact area keeps nearly the same as its initial value due to the low temperature rise as shown in Fig 6(a) at $x_R = \pm A$. The slight decrease of the contact area results in the increase of the maximum value of the contact pressure shown in Fig. 7(b), which in turn affects the contact temperature illustrated in Figs. 5 and 6. Since the total heat generated in the contact interface, evaluated by Eq. (6b), remains unchanged in comparison with the heat transfer analysis without thermaomechanical interaction, the thermal expansion has only little effect on the temperature in the half space solid. Such effects mainly focus in the contact region shown in Fig. 6(b) when the sphere oscillates to the locations near or at the oscillatory center shown in Fig. 6(a).

5.2. Case II. Oscillatory contact with the sphere fixed against displacement in vertical direction

Similar simulation as in Case I is performed, where the sphere oscillates along the x direction in contact with a semi-infinite solid, but the sphere is fixed against in vertical direction after pressed into the semi-infinite solid up to a very small specified depth. The indentation yields the same initial contact pressure as that in Case I and the same contact force $W_c = 1000$ N. The results are compared with those in Case I.

Fig. 8 shows the dimensionless temperature contour for Case II when the sphere oscillates from the left to the right relative to the neutral position. The same behaviors as those in Fig. 5 are observed in Fig. 8 but with a higher surface temperature. Fig. 9(a) presents the comparison of the surface temperature distributions between Case I and Case II when the sphere oscillates to the five different locations, $x_R = -A$, $-0.5A$, 0, $0.5A$, A, from the left to the right. Fig. 9(b) shows the effect of the thermal expansion in Case II on the temperature distribution compared with the temperature distribution in Case I and the result without TMC along the oscillatory direction when the sphere is at the oscillatory center. Figs. 8 and 9 illustrate that the thermal expansion in Case II affects the surface temperature in the entire region covered by the oscillatory sphere

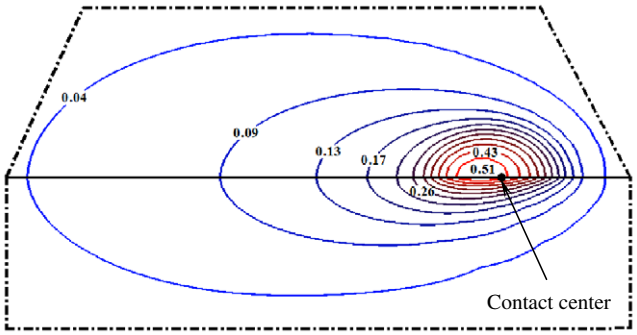

Fig. 8. Dimensionless temperature contour when the sphere oscillates to the oscillatory center from the left to the right for the oscillatory contact with the sphere fixed against displacement in vertical direction. The temperature is normalized by $2Rq_0/k$. R and q_0 are the initial contact radius and the initial average heat flux, respectively.

and such effect becomes more significant when the sphere oscillates close to the oscillatory center as shown in Figs. 8 and 9.

Fig. 10 shows the variation of the maximum contact pressure and the contact force with the dimensionless maximum contact temperature, respectively. The pressure is normalized by the initial maximum contact pressure p_{mi}, and the force by the initial contact force W_{ci}. Fig. 10(a) demonstrates a faster rate of increase in the peak contact pressure with the maximum contact temperature to

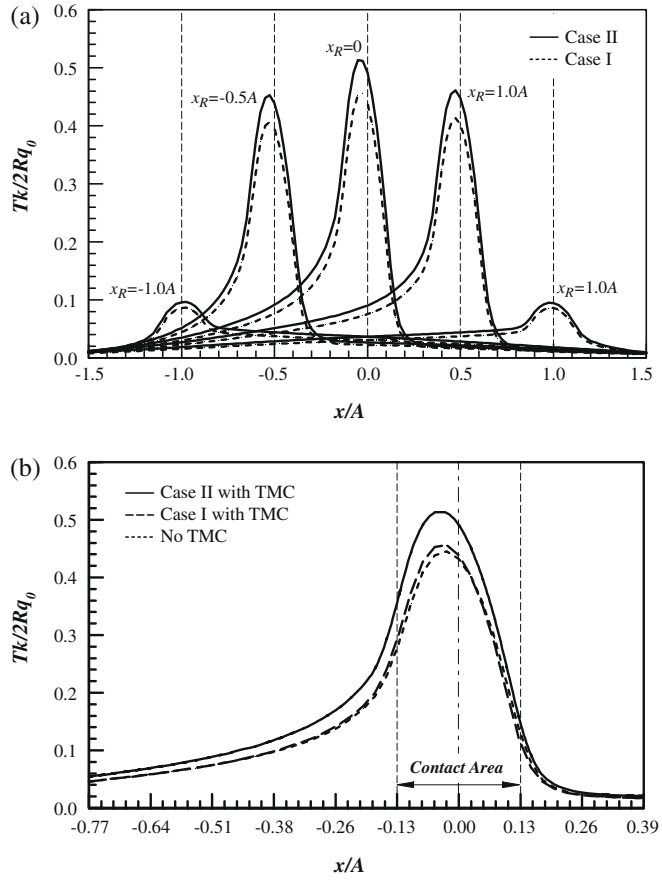

Fig. 9. Comparison of the surface temperature distributions between Case I and Case II along the sliding direction. (a) When the sphere/heat source is at the different locations. (b) When the sphere/heat source is at the oscillatory center. The origin is located at the neutral position of the oscillatory motion. q_0 is the initial average heat flux. A is the oscillatory amplitude.

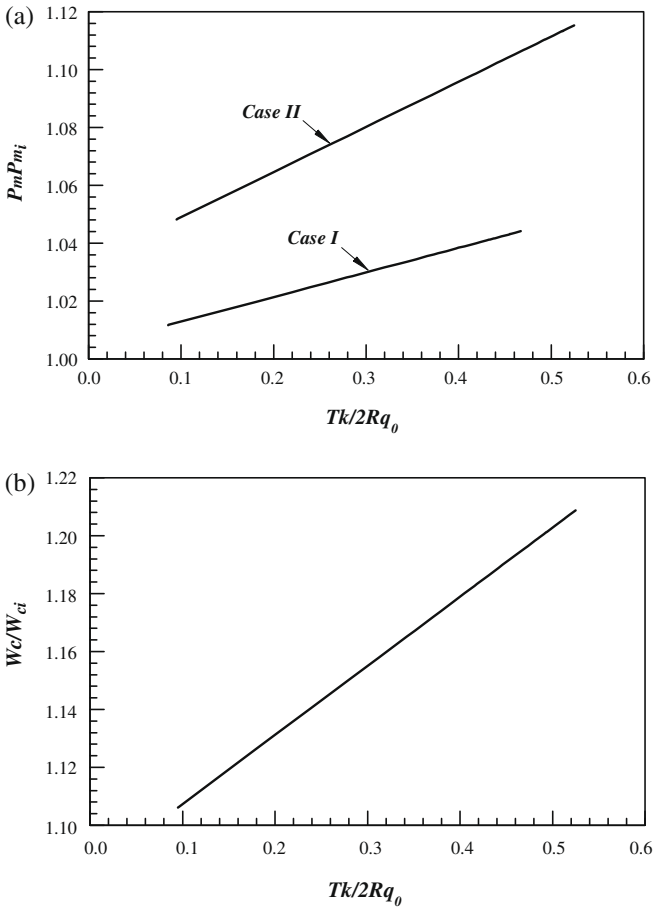

Fig. 10. Variation of (a) maximum contact pressure and (b) contact force with the dimensionless maximum contact temperature for the oscillatory contact with the sphere fixed against displacement in vertical direction in Case II. p_{mi} and W_{ci} is the initial indentation depth and the initial contact force, respectively. R and q_0 are the initial contact radius and the initial average heat flux, respectively.

greater values in Case II than in Case I. The thermal expansion in Case II additionally results in a significant increase of the contact force as revealed in Fig. 10(b). The increase of the contact force will results in an increase in the friction force, and thus an increase of the heat generation and the power loss.

For the case with sphere fixed against displacement in the vertical direction, the outward expansion of the contact surface due to the temperature rise tends to lift the sphere up and reduce the indentation depth in the half space. However, such a trend is constrained by the sphere, which is fixed against displacement in the vertical direction, resulting in the greater increase of the contact pressure shown in Fig. 10(a) and a concomitant rise in the contact force shown in Fig. 10(b). Also, the outward expansion of the contact surface due to the thermal expansion brings additional points on the half space surface in contact with the sphere and thus increases the contact area. The simulation results reveal that there is a maximum 4.4% increase of the contact area. Due to more significant increase of the contact force shown Fig. 10(b), the contact pressure and the heat generation increase greatly, resulting in a higher rise of the surface temperature.

Table 2 presents the comparison of the thermomechanical effects on the contact area, maximum contact pressure, contact force and temperature between Case I and Case II, where the values represent the increase percentage of the parameters by comparing with those obtained without consideration of the thermomechanical effects. Therefore, the negative contact area in Table 2 means a decrease in the contact area in Case I when compared with that

Table 2
Increase percentage of parameters with respect to those without thermoelastic effect.

	Contact area (%)	Max. contact pressure (%)	Max. contact force (%)	Max. temperature (%)
Case I	−3.8	4.8	0	2.1
Case II	+4.4	12.0	21.3	14.8

without the thermomechanical effects. It can be seen that the thermal expansion in Case II plays a significant role on the temperature rise, much more than that in Case I. Therefore, more care should be taken when the thermal expansion in an oscillatory contact is constrained due to the structural configuration of the system. For example, when dealing with journal bearings that experiences oscillatory motion, with the busing constrained by an external housing, the thermal expansion of the shaft and bushing could result in the loss of the clearance. A complete loss of the designed clearance between the shaft and bushing may occur with the catastrophic seizure [20,21].

In the above two cases, Cases I and II, the steady state for temperature can be reached. There also exist some other situations where a very large contact temperature is developed and that steady state temperature is not attained. The large temperature can be indicative of the possibility of scuffing failure [22,23], which may occur in the contacting bodies relatively oscillating at a high speed under heavy load. In Case II, when increasing the oscillatory frequency up to 13 Hz and keeping the rest operation parameters the same, the maximum contact temperature can rise to over 700 °C after four cycles. The contour for the absolute temperature is presented in Fig. 11, where the maximum temperature is 726 °C.

6. Conclusions

A thermomechanical model is developed to study the interaction of a semi-infinite elastic solid in contact with a rigid adiabatic sphere subjected to oscillatory sliding motion. The thermal and mechanical parts of the contact solution are treated independently and then combined together through a numerical iteration scheme to obtain a thermomechanical solution. In the presented simulations, the distribution of the transient temperature is calculated efficiently by the transfer matrix method. The model makes it practical to handle the problems involving thermomechanical interaction in oscillatory contacts, where simulations using the direct approach could become computationally prohibitive.

In the case of the oscillatory contact under a constant applied force, the thermal expansion due to the temperature rise in the half space results in an outward expansion of the contact surface. This expansion tends to lift the sphere up, reduces the indentation depth, and thus leads to a slight decrease of the contact area.

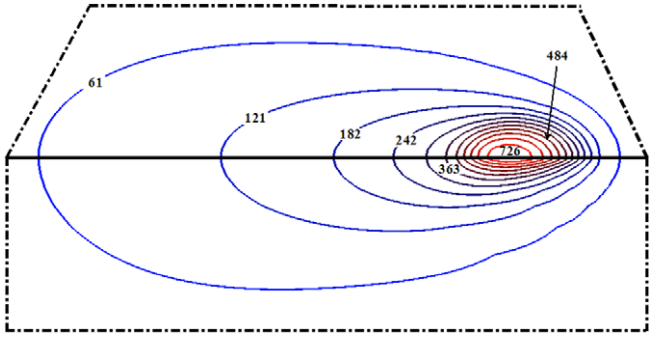

Fig. 11. Contour for the absolute temperature for the case of possible scuffing failure.

The slight decrease of the contact area results in the increase of the maximum value of the contact pressure and the change of the pressure distribution, which in turn affects the distribution of the heat flux and the temperature rise in the contact region. Since the total heat generated in the contact interface remains unchanged in comparison with the heat transfer without thermomechanical effects, the thermal expansion has only little effect on the temperature rise in the half space. Such effects mainly focus in the contact region when the sphere oscillates to the locations near or at the oscillatory center.

For the case of the oscillatory contact with the sphere fixed against direction in the indentation direction, the outward expansion of the contact surface due to the thermal expansion tends to lift the sphere up and reduce the indentation depth of the sphere into the half space. However, this trend is constrained by the sphere, which is fixed against in the indentation direction, resulting in the significant increase of the contact pressure and contact force. Also, the outward expansion of the contact surface due to the thermal expansion brings additional points on the half space surface in contact with the sphere and thus increases the contact area. Due to the significant increase of the contact force, the contact pressure and the heat generation increase greatly, resulting in the higher rise of the surface temperature.

Therefore, whether the thermal expansion in the contact components is constrained or not in the indentation direction plays a significant role in the thermaomechanical interaction in the oscillatory contact. Care should be taken when the thermal expansion in an oscillatory contact is constrained due to the structural configuration of the system to ensure that loss of clearance does not occur. This is a particularly important problem in journal bearings undergoing oscillatory motion with their bushings constrained by an external housing. Failure of proper consideration of thermomechanical interaction can result in a complete loss of the operating clearance and a catastrophic seizure.

References

[1] H. Blok, Theoretical study of temperature rise at surfaces of actual contact under oiliness conditions, Proc. Inst. Mech. Eng. 2 (1937) 222–235.
[2] J.C. Jaeger, Moving sources of heat and the temperature at sliding contacts, J. Proc. R. Soc. New South Wales 76 (1942) 203–224.
[3] X. Tian, F.E. Kennedy, Maximum and average flash temperature in sliding contacts, ASME J. Tribol. 116 (1994) 167–174.
[4] S.B. Liu, S. Lannou, Q. Wang, L. Keer, Solutions for temperature rise in stationary/moving bodies caused by surface heating with surface convection, ASME J. Tribol. 126 (2004) 776–785.
[5] F. Hirano, S. Yoshida, Theoretical study of temperature rise at contact surface for reciprocating motion, Am. Inst. Chem. Eng. 4 (1966) 127–132.
[6] J. Wen, M.M. Khonsari, Transient temperature involving oscillating heat source with application in fretting contact, ASME J. Tribol. 129 (2007) 517–527.
[7] Y. Ju, T.N. Farris, FFT thermomechanical solutions for moving heat sources, ASME J. Tribol. 119 (1997) 156–162.
[8] S.B. Liu, Q. Wang, Transient thermoelastic stress field in a half space, ASME J. Tribol. 125 (2003) 33–43.
[9] A. Martini, S.B. Liu, Q. Wang, Transient three-dimensional solution for thermoelastic displacement due to surface heating and convective cooling, ASME J. Tribol. 127 (2005) 750–755.
[10] Z.Q. Gong, K. Komvopoulos, Thermomechanical analysis of semi-infinite solid in sliding contact with a fractual surface, ASME J. Tribol. 127 (2005) 331–342.
[11] G. Liu, Q. Wang, Thermoelastic asperity contacts, frictional shear, and parameter correlations, ASME J. Tribol. 122 (2000) 300–307.
[12] G. Liu, Q. Wang, S.B. Liu, A three-dimensional thermo-mechanical asperity contact model for two nominal flat surfaces in contact, ASME J. Tribol. 123 (2001) 595–602.
[13] S.B. Liu, Q. Wang, A three-dimensional thermo-mechanical model of contact between two non-conformal rough surfaces, ASME J. Tribol. 123 (2001) 17–26.
[14] N. Ye, K. Komvopoulos, Three-dimensional finite element analysis of elastic–plastic layered media under thermomechaincal surface loading, ASME J. Tribol. 125 (2003) 52–59.
[15] Z.Q. Gong, K. Komvopoulos, Mechanical and thermomechanical elastic–plastic contact analysis of layered media with patterned surfaces, ASME J. Tribol. 126 (2004) 9–17.
[16] J. Wen, M.M. Khonsari, Transient heat conduction in rolling/sliding components by a dual reciprocity boundary element method, Int. J. Heat Mass Transfer 52 (2009) 1600–1607.

[17] G.E. Myers, Analytical Method in Conduction Heat Transfer, second ed., AMCHT Press, Madison, Wisconsin, 1998 (chapter 9).
[18] W.J. Minkowycz, E.M. Sparrow, J.Y. Murthy, Handbook of Numerical Heat Transfer, second ed., John Wiley & Sons Inc., Hoboken, New Jersey, 2006 (chapter 3).
[19] K.L. Johnson, Contact Mechanics, Cambridge University Press, UK, 1987 (chapter 4).
[20] M.M. Khonsari, H.J. Kim, On thermally induced seizure in journal bearings, ASME J. Tribol. 111 (1989) 661–667.
[21] T.L. Hazlett, M.M. Khonsari, Thermoelastic Behavior of Journal Bearing Undergoing Seizure – A Finite Element Study, M.S. thesis, University of Pittsburgh, Pittsburgh, PA, 1992.
[22] A. Dyson, L.D. Wedeven, Assessment of lubricated contacts – mechanism of scuffing and scoring, NASA Tech Memorandum 83074 (1983).
[23] M.J. Patching, C.C. Kweh, H.P. Evans, R.W. Snidle, Conditions for scuffing failure of ground and superfinished steel disk at high sliding speeds using a gas turbine engine oil, ASME J. Tribol. 117 (1995) 482–489.